Washington University School of Medicine

Digital Commons@Becker

5-1-2022

Three-dimensional quantification of cam resection using MRI bone models: A comparison of 2 techniques

Thomas D Alter
Rush University Medical Center

Derrick M Knapik
Washington University School of Medicine in St. Louis

Martina Guidetti
Rush University Medical Center

Alejandro Espinoza
Rush University Medical Center

Jorge Chahla
Rush University Medical Center

See next page for additional authors

Recommended Citation

Authors

Thomas D Alter, Derrick M Knapik, Martina Guidetti, Alejandro Espinoza, Jorge Chahla, Shane J Nho, and Philip Malloy

Three-Dimensional Quantification of Cam Resection Using MRI Bone Models

A Comparison of 2 Techniques

Thomas D. Alter,*[†] MS, Derrick M. Knapik,[‡] MD, Martina Guidetti,[†] PhD,
Alejandro Espinoza,[†] PhD, Jorge Chahla,[†] MD, PhD, Shane J. Nho,[†] MD, MS,
and Philip Malloy,[†§] PhD, PT
Investigation performed at Rush University Medical Center, Chicago, IL, USA

Background: The current clinical standard for the evaluation of cam deformity in femoroacetabular impingement syndrome is based on radiographic measurements, which limit the ability to quantify the complex 3-dimensional (3D) morphology of the proximal femur.

Purpose: To compare magnetic resonance imaging (MRI)–based metrics for the quantification of cam resection as derived using a best-fit sphere alpha angle (BFS-AA) method and using 3D preoperative-postoperative surface model subtraction (PP-SMS).

Study Design: Descriptive laboratory study.

Methods: Seven cadaveric hemipelvises underwent 1.5-T MRI before and after arthroscopic femoral osteochondroplasty, and 3D bone models of the proximal femur were reconstructed from the MRI scans. The alpha angles were measured radially along clockfaces using a BFS-AA method from the literature and plotted as continuous curves for the pre- and postoperative models. The difference between the areas under the curve for the pre- and postoperative models was then introduced in the current study as the BFS-AA–based metric to quantify the cam resection. The cam resection was also quantified using a 3D PP-SMS method, previously described in the literature using the metrics of surface area (FSA), volume (FV), and height (maximum [FH_{max}] and mean [FH_{mean}]). Bivariate correlation analyses were performed to compare the metrics quantifying the cam resection as derived from the BFS-AA and PP-SMS methods.

Results: The mean ± standard deviation maximum pre- and postoperative alpha angle measurements were 59.73° ± 15.38° and 48.02° ± 13.14°, respectively. The mean for each metric quantifying the cam resection with the PP-SMS method was as follows: FSA, 540.9 ± 150.7 mm^2; FV, 1019.2 ± 486.2 mm^3; FH_{max}, 3.6 ± 1.0 mm; and FH_{mean}, 1.8 ± 0.5 mm. Bivariate correlations between the BFS-AA–based and PP-SMS–based metrics were strong: FSA ($r = 0.817$, $P = .012$), FV ($r = 0.888$, $P = .004$), FH_{max} ($r = 0.786$, $P = .018$), and FH_{mean} ($r = 0.679$, $P = .047$).

Conclusion: Strong positive correlations were appreciated between the BFS-AA and PP-SMS methods quantifying the cam resection.

Clinical Relevance: The utility of the BFS-AA technique is primarily during preoperative planning. The utility of the PP-SMS technique is in the postoperative setting when evaluating the adequacy of resection or in patients with persistent hip pain with suspected residual impingement. In combination, the techniques allow surgeons to develop a planned resection while providing a means to evaluate the depth of resection postoperatively.

Keywords: femoroacetabular impingement syndrome; MRI; hip pain; 3D bone models; cam

Femoroacetabular impingement syndrome (FAIS) represents a structural abnormality of the hip at the articulation of the proximal femur and acetabulum, leading to altered contact forces at the joint level with resultant pain and injuries to the cartilage and labrum.[4,14,42,43] For patients with FAIS who have

symptoms, hip arthroscopy has been shown to yield successful outcomes for the treatment of intrapathologies.[1,16] However, certain patients may report recurrent symptoms and pain after primary hip arthroscopy, necessitating revision hip arthroscopy and hip preservation procedures.[7,10,45,50] Revision hip arthroscopy occurs in 5% to 14% of patients after the index surgical procedure, with multiple investigations citing inadequate bony resection, primarily of cam lesions, as the most common indication for revision.[10,13,43,45] While patient-

reported outcomes have demonstrated improvement after revision hip arthroscopy, outcomes are substantially lower when compared with those of patients undergoing primary hip arthroscopy.[13,48,50] Previous literature has noted the presence of high-grade chondral lesions in a majority of patients undergoing revision surgery secondary to inadequate bony resection at the index procedure, potentially accounting for the inferior outcomes in patients undergoing revision surgery.[23]

While underresection and residual cam impingement represent inadequate treatment of cam impingement, overresection of cam lesions reportedly increases the risk for femoral neck fracture[8,39] and may disrupt the labral suction seal properties of the hip, potentially causing iatrogenic instability of the hip.[2,27] The presence of persistent impingement or overresection after primary hip arthroscopy has been speculated to occur as a result of limited pre- and intraoperative imaging, leading surgeons to underappreciate the degree of anterosuperior bony overgrowth.[21,38]

While plain radiographs remain the clinical standard in screening for bony abnormalities in patients with FAIS,[5,20] radiographic measurements of cam deformity provide limited visualization of the complex 3-dimensional (3D) morphology of the hip joint.[37] Given the recognized limitations of 2-dimensional (2D) radiography, the incorporation of 3D methods to evaluate the hip joint has increased in popularity, improving characterization of deformity extent and location while aiding surgeons in determining appropriate cam resection.[37,47] In 2013, Kang et al[28] described the use of the best-fit sphere alpha angle (BFS-AA) method to characterize the size and location of cam deformity, demonstrating that 3D computed tomography (CT) could be used to define the boundaries of the cam deformity. Cong et al[12] evaluated the relationship of cam deformity between the best-fit sphere (BFS) method on 3D CT and reformatted oblique axial, oblique coronal, and radial views. The authors reported that the cam area displayed using the BFS method was greater than that evaluated on reformatted CT images, with the radial view demonstrating the greatest area among the sequences. Malloy et al[37] validated the use of magnetic resonance imaging (MRI) for evaluating the anatomy of the proximal femur in patients with cam-type FAIS, reporting that 1.5-T MRI produced femoral surface models that more accurately represented the actual bone surface than did CT with respect to the laser-scanned ground-truth models. More recently, Guidetti et al[22] incorporated postoperative imaging to quantify the amount of bone resected after osteochondroplasty via a 3D preoperative-postoperative surface model subtraction (PP-SMS) technique.

As the primary metric for evaluating the sphericity of the femoral head, alpha angle measurements have been established using multiple imaging modalities and views.[3,6,18,32,33] Given the complex 3D morphology associated with cam-type FAIS, multiple 2D views are necessary to accurately evaluate cam morphology in the assessment of patients with hip pain secondary to FAIS.[12,36,52] Increased accessibility of 1.5-T MRI scanners and advancements in imaging techniques have allowed for increased utility of MRI in the clinical setting, thereby eliminating the need for radiation exposure. Additionally, the ability to use MRI to assess soft tissue and bony anatomy has streamlined the preoperative workup by reducing the need for multiple diagnostic tests, with the added benefit of reducing cost. Advancements in commercial software allowing for the clinical application of 3D studies have opened the field for opportunities to generate new metrics to accurately quantify the 3D nature of bony deformities. However, the introduction of new metrics (ie, PP-SMS) requires comparison with the current standard (ie, the alpha angle). The purpose of the study was to compare MRI-based metrics for the quantification of cam resection as derived using a BFS-AA method and a 3D PP-SMS technique. We hypothesized that a strong association between BFS-AA and PP-SMS in quantifying the cam resection would be present.

METHODS

Specimen Selection

Seven fresh-frozen cadaveric hemipelvises with attached femur and intact hip capsules were procured from ScienceCare for this study. The inclusion criteria were cadavers with an alpha angle >50° on the axial slice of an MRI scan. The exclusion criteria were hips with evidence of previous surgical intervention performed on the pelvis or proximal femur, evidence of osteoarthritis (Tönnis grade >1), or history of metastatic cancer with osseous involvement. The mean ± standard deviation donor age and body mass index were 51.0 ± 12.5 years and 19.3 ± 3.6, respectively. All specimens were stored in a laboratory freezer at –20°C until approximately 48 hours before use and then thawed to room temperature for testing and imaging.[15,44] Institutional review board approval was not required for this study.

*Address correspondence to Thomas D. Alter, MS, Department of Orthopedic Surgery, Rush University Medical Center, 1611 W Harrison St, Chicago, IL 60612, USA (email: nho.research@rushortho.com).

†Section of Young Adult Hip Surgery, Division of Sports Medicine, Department of Orthopedic Surgery, Hip Preservation Center, Rush University Medical Center, Chicago, Illinois, USA.

‡Division of Sports Medicine, Department of Orthopedic Surgery, Washington University, St Louis, Missouri, USA.

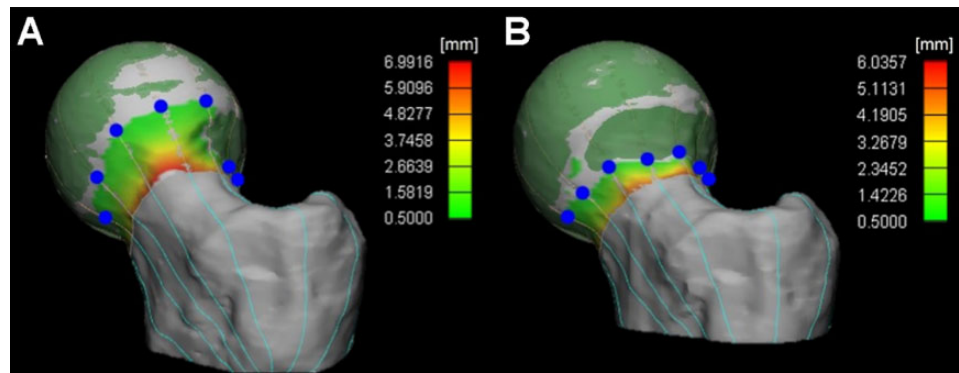§Arcadia University, Glenside, Pennsylvania, USA.

Figure 1. Alpha angle measured in 1-hour increments from 10 to 4 o'clock in the (A) pre- and (B) postoperative 3-dimensional models. Dark green represents the surface of the best-fit sphere to the femoral head. Light gray indicates where the femoral surface deviates from the best-fit sphere. The heat map quantifies the deviation in millimeters for the region where it exceeds the 0.5-mm set threshold. The blue points represent the boundary where the deviation exceeds 0.5 mm; therefore, they delineate the cam boundary in panel A. The blue points moved to different positions in panel B as the cam was resected during surgery.

Pre- and Postoperative MRI

Pre- and postoperative MRI scans were performed on all specimens on a 1.5-T Magnetom Espree system (Siemens) using a sequence previously described.[22,37] All MRI scans were exported as DICOM (Digital Imaging and Communication in Medicine) files and stored in an institutional picture archiving and communication system. All pre- and postoperative MRI scans were segmented using a semiautomatic segmentation process with commercially available software (Mimics version 21; Materialise). All segmentations were performed by a trained biomedical engineer (M.G.).

Hip Arthroscopy: Surgical Technique

Arthroscopic femoral osteochondroplasty was performed on all cadaveric specimens by a single fellowship-trained, high-volume hip arthroscopic surgeon (S.J.N.) in standard surgical fashion as previously described,[17,24] with a postoperative target alpha angle of 42°.[41]

BFS-AA Method

The alpha angles were measured radially on the pre- and postoperative 3D femoral bone models based on the femoral clockface from 10 to 4 o'clock in 1-hour increments using 3-matic 3D modeling software (Materialise) (Figure 1). Use of 1-hour increments (ie, 30° intervals) were based on previous literature.[31] The software reads the commonly used .STL format (Standard Tessellation Language), which describes the surface geometry of a 3D object. The surface of the femoral head and neck was manually selected from the 3D model, making sure to exclude the fovea capitis region for the selection of the femoral head surface. The surface selected for the femoral head region was fitted to a spherical surface, with the center of the BFS identifying the center of the femoral head. The center of the femoral neck was identified as the center of gravity of the surface selected as the femoral neck region. The alpha angle was defined as the angle between 2 lines originating at the center of the femoral head. Line 1 was taken as the femoral neck axis, which extended from the center of the femoral head to the center of gravity of the femoral neck. Line 2 extended from the center of the femoral head to the point at which the bone surface exceeded the surface of the BFS by 0.5 mm. A threshold of 0.5 mm was used to account for the mean segmentation error.[37]

Quantifying the Cam via the BFS-AA Method

The pre- and postoperative alpha angle measurements based on the 3D model, obtained along the femoral clockfaces using the BFS-AA method, were plotted as continuous curves. The areas under the curve (AUCs) for the pre- and postoperative alpha angles (AUCpreop and AUCpostop, respectively) were determined (Figure 2, A and B). The plots were then superimposed (Figure 2C), and the difference ($\Delta AUC = AUC_{preop} - AUC_{postop}$) was used to quantify the cam resection during the arthroscopic surgery (Figure 2D).

Quantifying the Cam via the 3D PP-SMS Technique

The postoperative 3D bone model was subtracted from the preoperative model to quantify the bone resected during hip arthroscopy as previously described.[22] The postoperative 3D bone model was subtracted from the preoperative model to quantify the bone resected during hip arthroscopy, with a threshold of greater than 0.5 mm (Figure 3) required to define the cam resection. The cam resection was quantified using the following metrics: maximum height (FH_{max}; mm), mean height (FH_{mean}; mm), surface area (FSA; mm^2), and volume (FV; mm^3).

Statistical Analysis

The primary dependent variables of interest were as follows: the metrics quantifying the cam resection (FH_{max}, FH_{mean}, FSA, FV) and the difference in the AUCs between pre- and postoperative alpha angles (ΔAUC). All data were inspected before analysis to determine if parametric
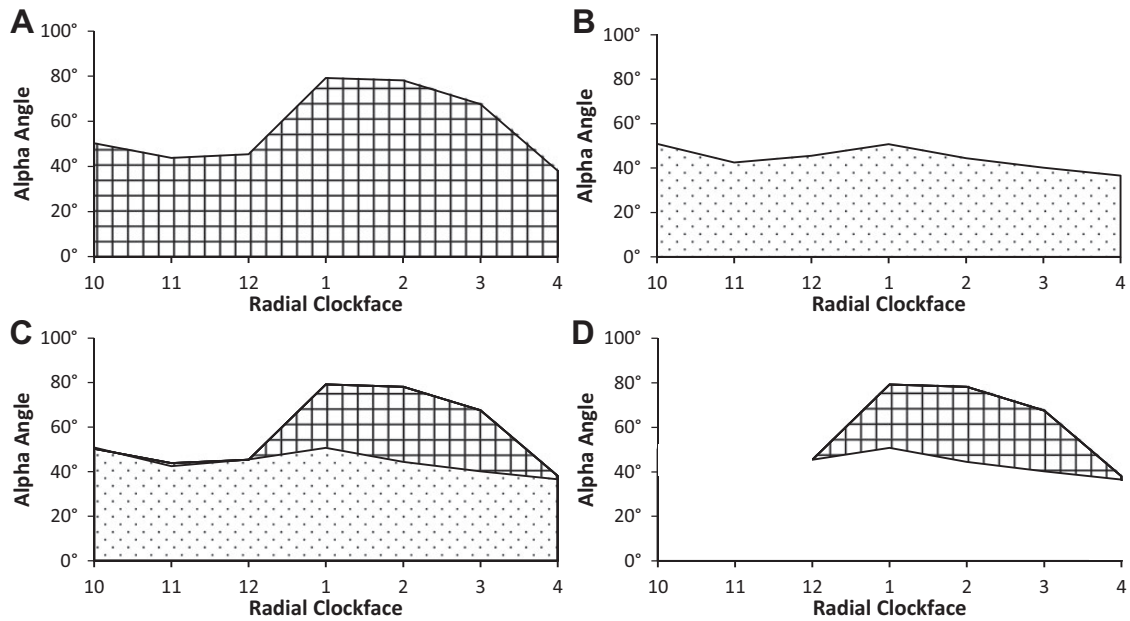
Figure 2. (A) Pre- and (B) postoperative alpha angle curve for the measurements performed on 3-dimensionally reconstructed hip bone models from 10 to 4 o'clock. The grid-like and dotted surfaces represent the areas under the curve for the pre- and postoperative alpha angles, respectively. (C) Superposition of the pre- and postoperative curve plots in panels A and B. (D) Difference between the areas under the pre- and postoperative curves quantifies the cam resection as the difference in bony morphology before and after surgery.
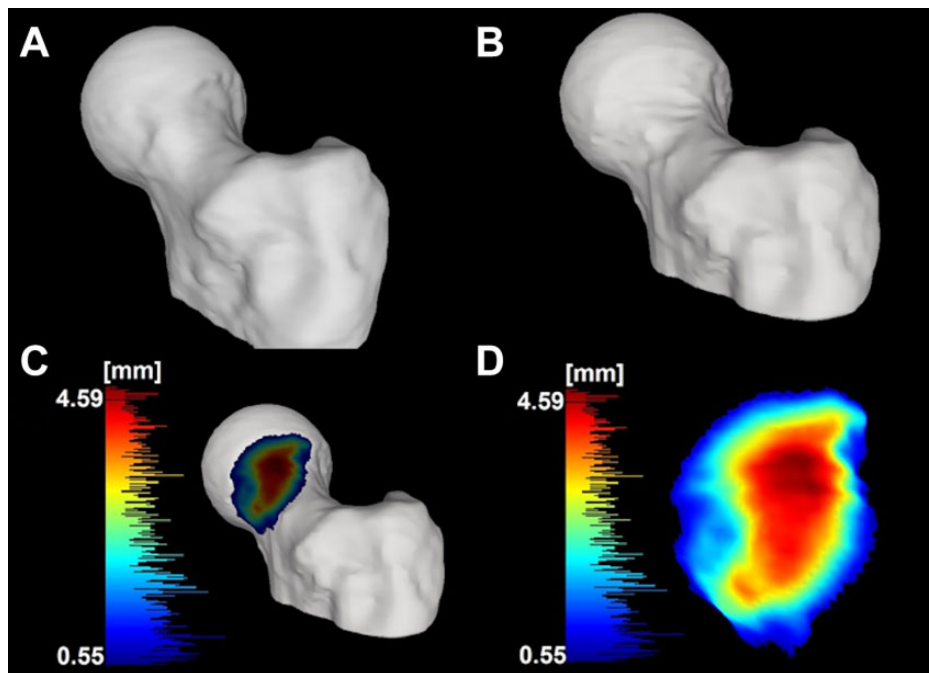
Figure 3. Example of the application of the preoperative-postoperative surface model subtraction technique. (A) Pre- and (B) postoperative models and (C) cam resection resulting from the subtraction of the latter from the former. A heat map of the height of the cam resection in millimeters is based on the surface-to-surface distance between the cam resection model and the postoperative bone model. The scale of the histogram has a lower threshold set at 0.5 mm (blue = minimal resection) with increasing depth (red = substantial resection). (D) Zoom-in of the cam resection with the same heat map scale in panel C.
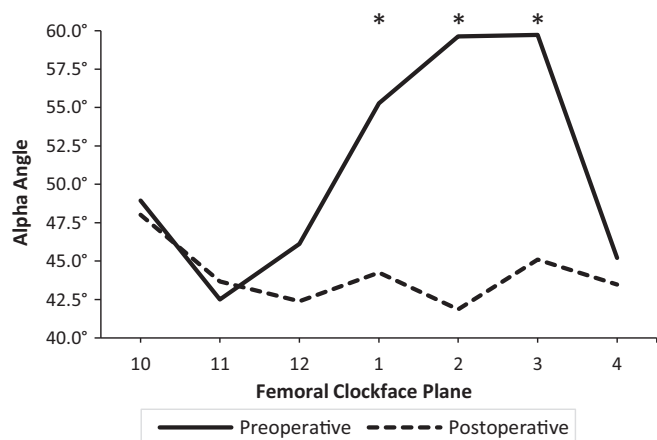
Figure 4. Mean pre- and postoperative alpha angle measurements based on the best-fit sphere alpha angle method for the 7 cadaveric specimens. *P < .05.

statistical analysis assumptions were met. The Shapiro-Wilk test was used to determine normality, and box plots were used to identify outliers. In the event of violation of parametric assumptions, nonparametric statistical analyses were performed for the considered variables. A paired-samples t test was used to compare the pre- and postoperative alpha angles. Bivariate correlation analyses were performed to determine the relationship between the metrics quantifying the cam deformity based on the BFS-AA and PP-SMS methods. The strength of the bivariate correlations was defined as follows: weak, 0.1 to 0.3; moderate, 0.3 to 0.5; and strong, 0.5 to 1.00.[11] All statistical analyses were performed using SPSS (Version 26; IBM Corp). An a priori α level was set at .05 to indicate statistical significance.

RESULTS

The mean pre- and postoperative alpha angles at each femoral clockface plane are displayed in Figure 4 as determined using the BFS-AA method. The mean maximum pre- and postoperative alpha angle measurements were 59.73° ± 15.38° and 48.02° ± 13.14°, respectively. There were significant reductions in alpha angle measurements at the 1-, 2-, and 3-o'clock femoral clockface planes after the arthroscopic femoral osteochondroplasty (P < .05) (Appendix Table A1). The mean for each PP-SMS–based metric quantifying the cam resection is displayed in Table 1.

Correlations Between Alpha Angle and Femoral Osteochondroplasty Metrics

Strong positive correlations were identified between the BFS-AA–based metric (ΔAUC) and all the PP-SMS–based metrics quantifying the cam resection (P < .05 for all) (Table 2). Scatterplots with a best-fit line were constructed between PP-SMS–based and BFS-AA–based metrics (Figure 5).

TABLE 1
Metrics Based on Preoperative-Postoperative Surface Model Subtraction[a]

Cam Resection	Mean ± SD (Range)
FH_{max}, mm	3.6 ± 1.0 (2.4-4.6)
FH_{mean}, mm	1.8 ± 0.5 (1.2-2.3)
FSA, mm^2	540.9 ± 150.7 (319.4-719.6)
FV, mm^3	1019.2 ± 486.2 (434.8-1551.4)

[a]FH_{max}, maximum height; FH_{mean}, mean height; FSA, surface area; FV, volume.

TABLE 2
Bivariate Correlations Between BFS-AA–Based and PP-SMS–Based Metrics[a]

Cam Resection	Correlation Coefficient	P
FH_{max}, mm	0.786	**.018**
FH_{mean}, mm	0.679	**.047**
FSA, mm^2	0.817	**.012**
FV, mm^3	0.888	**.004**

[a]Bold P values indicate statistical significance (P < .05). BFS-AA, best-fit sphere alpha angle; FH_{max}, maximum height; FH_{mean}, mean height; FSA, surface area; FV, volume; PP-SMS, preoperative-postoperative surface model subtraction.

DISCUSSION

The main findings from this in vitro cadaveric investigation were that the metrics quantifying cam resections based on MRI scans using the BFS-AA and PP-SMS methods were strongly correlated. The severity of cam morphology according to plain radiography is often determined using the magnitude of the alpha angle from a single radiographic 2D projection; however, this method often fails to reveal the extent of deformity, especially in cases when cam morphology extends distally along the neck. The BFS-AA method, which makes use of the radial alpha angles measured along the clockface, could be expanded for use in surgical planning by flattening the curve of the preoperative alpha angles to a target postoperative value.[41] The method provides a simplified way to quantify the full extent and location of the cam deformity that requires resection, emphasizing the necessity of evaluating all potential regions contributing to bony impingement along the femoral head and neck to minimize the rate of revision arthroscopy owing to inadequate surgical correction.

The frequency of insufficient or excessive cam resection is well established and often attributed to error in recognition or extent of decompression.[36] While sports medicine fellowships have improved training in hip arthroscopy, Gordon et al[19] reported a 64-fold difference in exposure among fellowship programs. Moreover, higher rates of revision surgery have been observed among surgeons performing a low volume of hip arthroscopy,[30,38] likely owing to the significant learning curve associated with hip arthroscopy.[9,29,49] Interactive computer vision interface (CVI)
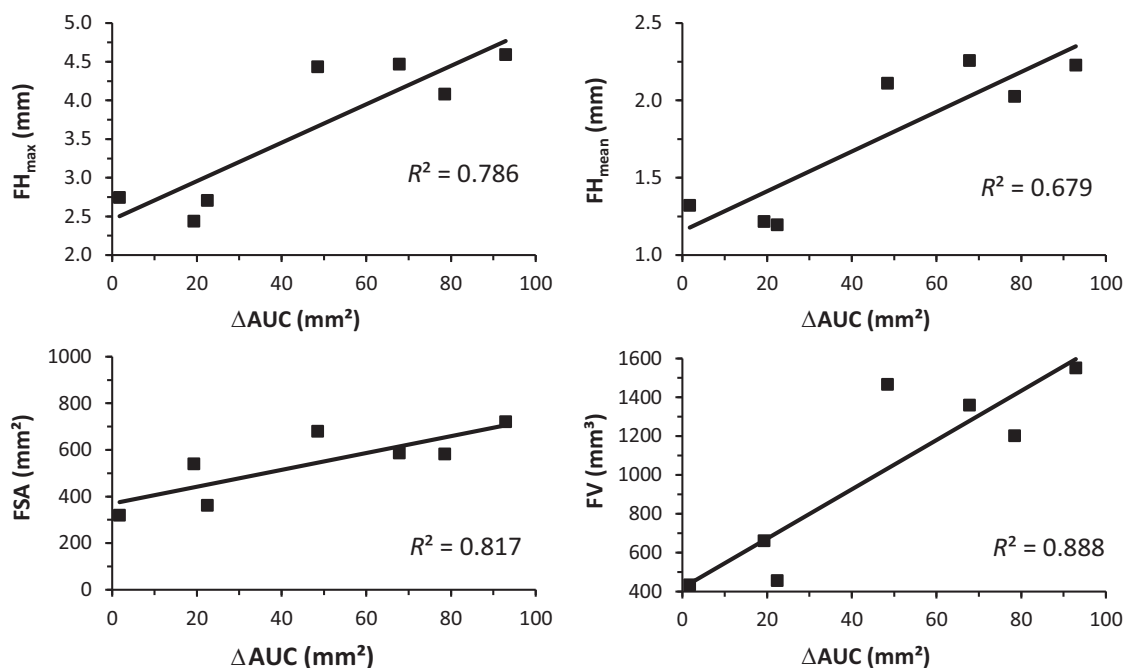
Figure 5. Scatterplots of significant correlations between metrics based on the best-fit sphere alpha angle method and preoperative-postoperative surface model subtraction technique. AUC, area under the curve; FH_{max}, maximum height; FH_{mean}, mean height; FSA, surface area; FV, femoroplasty volume.

programs have recently been introduced, making use of multiple fluoroscopic views to ensure complete bony resection. Looney et al[36] evaluated the use of CVI-guided femoroplasty in 102 hips with FAIS (51 hips treated with CVI, 51 treated without it). Using plain radiography as the reference standard, the authors noted that CVI more reliably detected cam deformities at the 12:30 and 1:45 views when compared with the 11:45 view. In addition, the authors stated that the strength of the correlation between CVI views and clinic radiographs was moderate at best, suggesting that improvements in diagnostics may be obtained using advanced imaging modalities incorporating radial cuts.[46]

In the present study, the 3D bone model–based metrics obtained using the PP-SMS technique demonstrated FH_{max} and FH_{mean} of 3.6 ± 1.0 mm and 1.8 ± 0.5 mm, respectively, while the FSA resected was 540.9 ± 150.7 mm[2]. These results are comparable to the metrics of cam morphology obtained using alternative techniques.[12,25,28] Kang et al[28] used a BFS method to describe cam morphology in 5 patients and reported a mean deformity height ranging from 0.78 to 2.65 mm. In a series of 26 patients with cam deformity, Cong et al[12] used the BFS method to quantify cam surface area and cited a mean area of 329.75 ± 42.7 mm.[2] Harris et al[25] used statistical shape modeling on CT-based 3D bone models between patients with FAIS and control participants to evaluate morphologic differences. They found that the mean cam protruded above the control mean by a maximum of 3.3 mm, with a sustained protrusion of 2.5 to 3.0 mm along the anterolateral head-neck junction. Despite providing valuable data on the 3D

quantitation of cam morphology, the aforementioned techniques do not quantify the actual extent of cam resection.

More recently, Guidetti et al[22] compared pre- and postoperative surface models and provided new metrics (ie, FH_{max}, FH_{mean}, FSA, FV) of quantifying bone resection during femoral osteochondroplasty. In the present study, the BFS method was used to quantify cam resection, with the ultimate goal of relating these metrics to those presented by Guidetti et al. The BFS-AA and PP-SMS metrics indicated strong positive correlations, with *r* values ranging from 0.679 to 0.888. A proportion of the variation of these results may be explained by the idealization of the femoral head as a perfect sphere. In a study by Harris et al,[26] the femoral head of 3D reconstructed bone models (n = 15 cam, n = 15 controls) was fit to ideal geometries consisting of rotational conchoids and spheres. According to the authors, conchoids provided a significantly better fit to native femoral head geometry than did spheres for both groups, and femurs with cam deformities demonstrated greater maximum deviations as compared with controls for sphere and conchoids.

The utility of the BFS-AA technique is primarily in preoperative planning. This method provides not only an improved understanding of the extent and magnitude of the patient's cam lesion based on the alpha angle measurements but also the depth of resection required to restore the abnormal bony morphology. This technique may prove advantageous given the known sex differences in femoral head size, with male patients having larger femoral heads, and therefore may require a greater depth of resection per degree change in alpha angle measurements when

compared with female patients.[54,56] The utility of the PP-SMS technique is in the postoperative setting when evaluating the adequacy of resection or in patients with residual hip pain. For patients with persistent pain and suspected residual impingement, postoperative MRI can be conducted to evaluate the actual depth of resection performed during surgery. This may help differentiate bony versus soft tissue causes of pain. Additionally, modifications to the preoperative bone model using techniques such as shape fitting have potential to generate a target postoperative bone model to allow the PP-SMS to also be used for preoperative planning. Future studies may focus on developing these techniques to be used in the clinic and to evaluate the relationship between 3D parameters and clinical outcomes.

Limitations

This study was not without limitations. Standard anteroposterior and Dunn lateral radiographs of the hip specimens were not obtained before osteochondroplasty, limiting comparison of clinical alpha angle measurements on radiographs with measurements obtained from MRI scans. While radiography is part of the standard workup in the patient with FAIS who has symptoms, MRI allows for assessment of cam resection, which is not capable of being measured on 2D radiographs. The sample size in this in vitro study was relatively small (n = 7), increasing the potential for type II statistical error attributed to being underpowered. However, the sample size in the current study is consistent with that of similar in vitro cadaveric investigations.[34,35,40,51,55] Additionally, the parametric tests in this study have been shown to be applicable with studies consisting of sample sizes ≤5.[53] Current technology requires pre- and postoperative MRI models, limiting the clinical utility as postoperative MRI is not standard of care. Although currently beyond our current technologic capabilities, advancements in shape-fitting techniques may allow for clinically applicable preoperative planning, facilitating identification of high-risk regions for impingement. Additionally, advancements in imaging techniques and automatization of bone model segmentation could ultimately allow this technique to be used in the operative setting after osteochondroplasty to confirm complete resection of abnormal bony morphology.

CONCLUSION

Strong positive correlations were appreciated between the BFS-AA and PP-SMS methods quantifying the cam resection. The utility of the BFS-AA technique is primarily during preoperative planning. The utility of the PP-SMS technique is in the postoperative setting when evaluating the adequacy of resection or in patients with persistent hip pain with suspected residual impingement. In combination, the techniques allow surgeons to develop a planned resection while providing a means to evaluate the depth of resection postoperatively.

REFERENCES

1. Alradwan H, Philippon MJ, Farrokhyar F, et al. Return to preinjury activity levels after surgical management of femoroacetabular impingement in athletes. *Arthroscopy*. 2012;28(10):1567-1576.
2. Arner JW, Ruzbarsky JJ, Soares R, Briggs K, Philippon MJ. Salvage revision hip arthroscopy including remplissage improves patient-reported outcomes after cam over-resection. *Arthroscopy*. 2021; 37(9):2809-2816.
3. Audenaert EA, Baelde N, Huysse W, Vigneron L, Pattyn C. Development of a three-dimensional detection method of cam deformities in femoroacetabular impingement. *Skeletal Radiol*. 2011;40(7):921-927.
4. Ayeni OR. In femoroacetabular impingement syndrome, hip arthroscopy improved hip-related quality of life at 12 months compared with conservative care. *J Bone Joint Surg Am*. 2019;101(4):371.
5. Barton C, Salineros MJ, Rakhra KS, Beaule PE. Validity of the alpha angle measurement on plain radiographs in the evaluation of cam-type femoroacetabular impingement. *Clin Orthop Relat Res*. 2011; 469(2):464-469.
6. Beaule PE, Zaragoza E, Motamedi K, Copelan N, Dorey FJ. Three-dimensional computed tomography of the hip in the assessment of femoroacetabular impingement. *J Orthop Res*. 2005;23(6):1286-1292.
7. Bogunovic L, Gottlieb M, Pashos G, Baca G, Clohisy JC. Why do hip arthroscopy procedures fail? *Clin Orthop Relat Res*. 2013;471(8): 2523-2529.
8. Bonano JC, Johannsen A, Mardones RM, et al. The effect of resection size in the treatment of cam-type femoroacetabular impingement in the typical patient with hip arthroscopy: a biomechanical analysis. *Am J Sports Med*. 2020;48(12):2897-2902.
9. Buyukdogan K, Utsunomiya H, Bolia I, et al. Right versus left hip arthroscopy for surgeons on the learning curve. *Arthrosc Tech*. 2017;6(5):e1837-e1844.
10. Clohisy JC, Nepple JJ, Larson CM, et al. Persistent structural disease is the most common cause of repeat hip preservation surgery. *Clin Orthop Relat Res*. 2013;471(12):3788-3794.
11. Cohen J. *Statistical Power Analysis for the Behavioral Sciences*. 2nd ed. Taylor & Francis; 1988.
12. Cong S, Liu S, Xie Y, Luo Z, Chen J. Evaluation of cam deformity on 3-dimensional computed tomography with the best-fit sphere technique and the alpha angle marking method. *Am J Sports Med*. 2021;49(4):1023-1030.
13. Cvetanovich GL, Harris JD, Erickson BJ, et al. Revision hip arthroscopy: a systematic review of diagnoses, operative findings, and outcomes. *Arthroscopy*. 2015;31(7):1382-1390.
14. de Sa D, Cargnelli S, Catapano M, et al. Femoroacetabular impingement in skeletally immature patients: a systematic review examining indications, outcomes, and complications of open and arthroscopic treatment. *Arthroscopy*. 2015;31(2):373-384.
15. Dirim B, Haghighi P, Trudell D, Portes G, Resnick D. Medial patellofemoral ligament: cadaveric investigation of anatomy with MRI, MR arthrography, and histologic correlation. *AJR Am J Roentgenol*. 2008; 191(2):490-498.
16. Domb BG, Gui C, Hutchinson MR, et al. Clinical outcomes of hip arthroscopic surgery: a prospective survival analysis of primary and revision surgeries in a large mixed cohort. *Am J Sports Med*. 2016; 44(10):2505-2517.
17. Frank RM, Lee S, Bush-Joseph CA, et al. Improved outcomes after hip arthroscopic surgery in patients undergoing T-capsulotomy with complete repair versus partial repair for femoroacetabular impingement: a comparative matched-pair analysis. *Am J Sports Med*. 2014; 42(11):2634-2642.
18. Golfam M, Di Primio LA, Beaule PE, Hack K, Schweitzer ME. Alpha angle measurements in healthy adult volunteers vary depending on the MRI plane acquisition used. *Am J Sports Med*. 2017;45(3): 620-626.
19. Gordon AM, Flanigan DC, Malik AT, Vasileff W. Orthopaedic surgery sports medicine fellows see substantial increase in hip arthroscopy procedural volume with high variability from 2011 to 2016. *Arthroscopy*. 2021;37(2):521-527.

20. Griffin DR, Dickenson EJ, O'Donnell J, et al. The Warwick Agreement on femoroacetabular impingement syndrome (FAI syndrome): an international consensus statement. *Br J Sports Med*. 2016;50(19):1169-1176.

21. Griffin JW, Weber AE, Kuhns B, Lewis P, Nho SJ. Imaging in hip arthroscopy for femoroacetabular impingement: a comprehensive approach. *Clin Sports Med*. 2016;35(3):331-344.

22. Guidetti M, Malloy P, Alter TD, et al. MRI- and CT-based metrics for the quantification of arthroscopic bone resections in femoroacetabular impingement syndrome. *J Orthop Res*. Published online June 30, 2021. doi:10.1002/jor.25139

23. Gwathmey FW, Jones KS, Thomas Byrd JW. Revision hip arthroscopy: findings and outcomes. *J Hip Preserv Surg*. 2017;4(4):318-323.

24. Harris JD, Slikker W III, Gupta AK, McCormick FM, Nho SJ. Routine complete capsular closure during hip arthroscopy. *Arthrosc Tech*. 2013;2(2):e89-e94.

25. Harris MD, Datar M, Whitaker RT, et al. Statistical shape modeling of cam femoroacetabular impingement. *J Orthop Res*. 2013;31(10):1620-1626.

26. Harris MD, Reese SP, Peters CL, Weiss JA, Anderson AE. Three-dimensional quantification of femoral head shape in controls and patients with cam-type femoroacetabular impingement. *Ann Biomed Eng*. 2013;41(6):1162-1171.

27. Hunt SA. Hip cam overresection may result in inferior outcomes: the Goldilocks paradox of too little, too much, or just right? Editorial commentary. *Arthroscopy*. 2021;37(9):2817-2819.

28. Kang RW, Yanke AB, Espinoza Orias AA, Inoue N, Nho SJ. Emerging ideas: novel 3-D quantification and classification of cam lesions in patients with femoroacetabular impingement. *Clin Orthop Relat Res*. 2013;471(2):358-362.

29. Kautzner J, Zeman P, Stancak A, Havlas V. Hip arthroscopy learning curve: a prospective single-surgeon study. *Int Orthop*. 2018;42(4):777-782.

30. Kester BS, Capogna B, Mahure SA, et al. Independent risk factors for revision surgery or conversion to total hip arthroplasty after hip arthroscopy: a review of a large statewide database from 2011 to 2012. *Arthroscopy*. 2018;34(2):464-470.

31. Khan O, Witt J. Evaluation of the magnitude and location of cam deformity using three dimensional CT analysis. *Bone Joint J*. 2014;96B(9):1167-1171.

32. Kobayashi N, Sumi K, Higashihira S, et al. Correlations and reproducibility between radiographic and radial alpha angles in the evaluation of cam morphology. *Orthop J Sports Med*. 2020;8(7):2325967120932922.

33. Konan S, Rayan F, Haddad FS. Is the frog lateral plain radiograph a reliable predictor of the alpha angle in femoroacetabular impingement? *J Bone Joint Surg Br*. 2010;92(1):47-50.

34. Lockard CA, Stake IK, Brady AW, et al. Accuracy of MRI-based talar cartilage thickness measurement and talus bone and cartilage modeling: comparison with ground-truth laser scan measurements. *Cartilage*. Published online December 3, 2020. doi:10.1177/1947603520976774

35. Logishetty K, van Arkel RJ, Ng KCG, et al. Hip capsule biomechanics after arthroplasty: the effect of implant, approach, and surgical repair. *Bone Joint J*. 2019;101B(4):426-434.

36. Looney AM, Wichman DM, Parvaresh KC, Alter TD, Nho SJ. Intraoperative computer vision integrated interactive fluoroscopy correlates with successful femoroplasty on clinic-based radiographs. *Arthroscopy*. Published online May 3, 2021. doi:10.1016/j.arthro.2021.04.044

37. Malloy P, Gasienica J, Dawe R, et al. 1.5 T magnetic resonance imaging generates accurate 3D proximal femoral models: surgical planning implications for femoroacetabular impingement. *J Orthop Res*. 2020;38(9):2050-2056.

38. Mehta N, Chamberlin P, Marx RG, et al. Defining the learning curve for hip arthroscopy: a threshold analysis of the volume-outcomes relationship. *Am J Sports Med*. 2018;46(6):1284-1293.

39. Merz MK, Christoforetti JJ, Domb BG. Femoral neck fracture after arthroscopic femoroplasty of the hip. *Orthopedics*. 2015;38(8):e696-e700.

40. Neubert A, Wilson KJ, Engstrom C, et al. Comparison of 3D bone models of the knee joint derived from CT and 3 T MR imaging. *Eur J Radiol*. 2017;93:178-184.

41. Notzli HP, Wyss TF, Stoecklin CH, et al. The contour of the femoral head-neck junction as a predictor for the risk of anterior impingement. *J Bone Joint Surg Br*. 2002;84(4):556-560.

42. Nwachukwu BU, Rebolledo BJ, McCormick F, et al. Arthroscopic versus open treatment of femoroacetabular impingement: a systematic review of medium- to long-term outcomes. *Am J Sports Med*. 2016;44(4):1062-1068.

43. O'Connor M, Steinl GK, Padaki AS, et al. Outcomes of revision hip arthroscopic surgery: a systematic review and meta-analysis. *Am J Sports Med*. 2020;48(5):1254-1262.

44. Poon S, Chen YH, Wendolowski SF, et al. Cadaveric study of the safety and device functionality of magnetically controlled growing rods after exposure to magnetic resonance imaging. *Spine Deform*. 2018;6(3):290-298.

45. Ross JR, Larson CM, Adeoye O, Kelly BT, Bedi A. Residual deformity is the most common reason for revision hip arthroscopy: a three-dimensional CT study. *Clin Orthop Relat Res*. 2015;473(4):1388-1395.

46. Saito M, Tsukada S, Yoshida K, Okada Y, Tasaki A. Correlation of alpha angle between various radiographic projections and radial magnetic resonance imaging for cam deformity in femoral head-neck junction. *Knee Surg Sports Traumatol Arthrosc*. 2017;25(1):77-83.

47. Samim M, Eftekhary N, Vigdorchik JM, et al. 3D-MRI versus 3D-CT in the evaluation of osseous anatomy in femoroacetabular impingement using Dixon 3D FLASH sequence. *Skeletal Radiol*. 2019;48(3):429-436.

48. Sardana V, Philippon MJ, de Sa D, et al. Revision hip arthroscopy indications and outcomes: a systematic review. *Arthroscopy*. 2015;31(10):2047-2055.

49. Schuttler KF, Schramm R, El-Zayat BF, et al. The effect of surgeon's learning curve: complications and outcome after hip arthroscopy. *Arch Orthop Trauma Surg*. 2018;138(10):1415-1421.

50. Shapira J, Kyin C, Go C, et al. Indications and outcomes of secondary hip procedures after failed hip arthroscopy: a systematic review. *Arthroscopy*. 2020;36(7):1992-2007.

51. Suppauksorn S, Beck EC, Rasio J, et al. A cadaveric study of cam-type femoroacetabular impingement: biomechanical comparison of contact pressures between cam morphology, partial femoral osteoplasty, and complete femoral osteoplasty. *Arthroscopy*. 2020;36(9):2425-2432.

52. Uemura K, Atkins PR, Anderson AE, Aoki SK. Do your routine radiographs to diagnose cam femoroacetabular impingement visualize the region of the femoral head-neck junction you intended? *Arthroscopy*. 2019;35(6):1796-1806.

53. Winter J. Using the Student's "t"-test with extremely small sample sizes. *Pract Assess Res Eval*. 2013;18:10.

54. Yanke AB, Khair MM, Stanley R, et al. Sex differences in patients with cam deformities with femoroacetabular impingement: 3-dimensional computed tomographic quantification. *Arthroscopy*. 2015;31(12):2301-2306.

55. Yanke AB, Shin JJ, Pearson I, et al. Three-dimensional magnetic resonance imaging quantification of glenoid bone loss is equivalent to 3-dimensional computed tomography quantification: cadaveric study. *Arthroscopy*. 2017;33(4):709-715.

56. Zhang L, Wells JE, Dessouky R, et al. 3D CT segmentation of CAM type femoroacetabular impingement-reliability and relationship of CAM lesion with anthropomorphic features. *Br J Radiol*. 2018;91(1092):20180371.

APPENDIX

APPENDIX TABLE A1
Mean Pre- and Postoperative Alpha Angle[a]

Location, Clockface	Alpha Angle, deg		P
	Preoperative	Postoperative	
10 o'clock	49.0 ± 7.6	48.0 ± 6.4	.155
11 o'clock	42.5 ± 2.7	43.7 ± 4.0	.113
12 o'clock	46.1 ± 12.0	42.4 ± 2.8	.433
1 o'clock	55.3 ± 15.4	44.3 ± 6.0	**.034**
2 o'clock	59.6 ± 12.0	41.9 ± 7.4	**.004**
3 o'clock	59.7 ± 7.7	45.1 ± 13.1	**.022**
4 o'clock	45.2 ± 4.2	43.5 ± 10.6	.373

[a]Data are presented as mean ± SD. Bold P values indicate statistically significant difference between pre- and postoperative ($P < .05$, paired t test).